The Characteristics and Suppression Protection Measures of AC Filter Closing Inrush Current Considering Residual Voltage and Residual Charge

Hongguang Gao

Abstract—In recent years, China has implemented numerous ultra-high voltage direct current transmission projects, offering notable advantages such as high stability, low losses, and cost-effectiveness. These projects necessitate frequent switching of AC filters at converter stations to meet reactive power requirements. During filter switching, a substantial closing inrush current is generated. The capacitors in AC filters, made up of multiple small capacitors in series and parallel, can retain residual charge and voltage if flashovers occur in some capacitors. Moreover, due to the capacitors' memory effect, rapid re-closing of the AC filter shortly after system operation can result in residual voltage, leading to a larger closing inrush current. This study presents a residual charge calculation model for high-voltage capacitors and a residual voltage model for quick re-closing scenarios established through PSCAD/EMTDC simulations. The research not only analyzes the detrimental effects of closing inrush current and overvoltage on the filter system caused by residual charges and voltage but also proposes innovative solutions with practical implications. To expedite the discharge of capacitors with residual charges, a novel adjustable discharge resistance model is proposed, which can enhance discharge speed by four times, significantly improving the efficiency and safety of high-voltage transmission systems. In addition, this paper introduces a new type of capacitor flashover fault identification method, which can achieve more accurate identification of the fault location and the number of capacitors that flashover occurs, thereby significantly facilitating the maintenance and troubleshooting of high-voltage systems.

Index Terms—AC filter, closing inrush current, closing resistance, residual charge

I. Introduction

THE proposal of 'carbon peak, carbon neutrality' entails the development of a clean, low-carbon, safe, and efficient energy system. This involves controlling the total amount of fossil energy, enhancing utilization efficiency, replacing traditional fossil energy with renewable energy sources, deepening power system reform, and establishing a new power system centered around new energy sources. By implementing critical decisions and action plans by leading enterprises in relevant industries, energy conservation, emission reduction, and the integration of new energy sources within the power system are expected to accelerate. This will lead to significant growth in the ultra-high voltage market. Converter stations, as vital components, play a crucial role in operating and maintaining ultra-high voltage converter stations, and their involvement is key to achieving the objective of 'carbon peaking and carbon neutrality.

This article delves into the significant research on the Changji Guquan ultra-high voltage direct current (UHVDC) transmission project. This project, which employs a bipolar single-circuit direct current transmission system with a rated voltage of 1100 kV and a rated current of 5455 A, operating on a 750 kV AC system, is a crucial advancement in the field. Installing of numerous filters within the converter station in high-voltage direct current transmission systems is a key aspect of this project. These filters play a vital role in compensating for substantial reactive power consumption, a critical function that ensures system's smooth operation, reducing harmonic components entering the AC system and preventing the AC bus voltage distortion rate from exceeding specified limits [1-8].

The AC filter in the converter station, primarily composed of filter inductance, filter capacitor, and filter resistor, is a key component that suppresses system noise generated within the converter station. It eliminates high-frequency noise, electromagnetic radiation, and other interference signals, ensuring the system's smooth and stable operation. Notably, when the filter is rapidly opened and closed, the capacitor components within the filter exhibit a memory effect, influencing the magnitude of the closing inrush current upon subsequent closure. To address this, a closing resistor is integrated within the filter. Reference [9] examined the internal structure of the closing resistor in a circuit breaker and established the distributed capacitance parameters of the closing resistor. Also, the voltage distribution characteristics between the closing resistor and the insulation rod in the presence of non-uniform stray capacitance were examined, and an enhanced closing resistor process was suggested in this reference. Reference [10] analyzed the transient waveform during the circuit breaker's closing process, utilized acoustic and vibration signals and physical field simulation to identify

Manuscript received January 2, 2024; revised October 17, 2024.

Hongguang Gao is a postgraduate of Key Laboratory of Modern Power System Simulation and Control & Renewable Energy Technology Ministry of Education, Northeast Electric Power University, Jilin 132012, China. (corresponding author e-mail: 13664351290@163.com).

abnormal operations due to closing resistor defects, and proposed improvement measures for potential defects in circuit breakers with closing resistor configurations. References [11-12] investigated the fault of the closing resistor contact in a specific circuit breaker, proposed a fault prediction method, and emphasized the significance of maintaining and managing the closing resistor.

Furthermore, deploying phase selection and closing devices can help mitigate closing inrush currents [13-17]. References [18-21] introduced the concept of residual charge, which is the charge that remains in a capacitor after it has been disconnected from its charging source. They explained its origin, established a model, and discussed associated hazards. They also emphasized the importance of promptly discharging capacitors to address residual charge. References [22] proposed two methods to enhance the capacitor discharge rate by increasing discharge current and adjusting resistance values, aiming to reduce discharge time significantly. To improve the efficiency of the discharge process, this paper introduces a new adjustable dynamic discharge resistor model. References [23-24] utilized electromagnetic transient simulation software to analyze the impact of switching on closing inrush current in 750 kV AC filters, suggesting appropriate measures for suppressing closing inrush current. The residual voltage on the capacitors in the filter can affect the closing inrush current during subsequent switching moments, a topic with limited domestic and international research. This study aims to simulate the residual voltage in the filter by applying voltages of 200 kV, 400 kV, and 612 kV to the capacitors. The impact on the operational stability of the filter components will be assessed by comparing the closing inrush current with and without residual voltage. Analyzing the changes in phase selection and closing resistance measures based on residual voltage will help identify the most effective method to suppress closing inrush current, highlighting the need for further research in this critical area.

II. Principle of Closing Inrush Current Generation

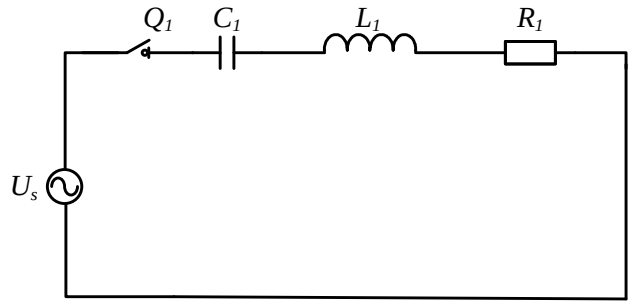

Fig. 1. Internal structure diagram of the filter.

During the switching process of the filter, transient components with high-frequency harmonics may lead to overvoltage of the main capacitor and overcurrent in the circuit. This phenomenon, known as closing inrush current, is primarily caused by the capacitive inductance of the AC filter. The interaction between the inductance and capacitive elements results in induced currents and reverse electromotive forces, forming the closing inrush current. This current, if not managed effectively, can significantly impact the safety and stability of the system. The urgency of controlling this phenomenon effectively cannot be overstated. For instance, in a single-tuned filter comprised of RLC components connected in series as depicted in Fig. 1, the calculation of closing inrush current involves a detailed process.

According to the RLC series second-order circuit, at the moment of circuit breaker closing:

$$\begin{cases} i = C\dfrac{dU_C}{dt} \\ iR + L\dfrac{di}{dt} + \dfrac{1}{C}\int i dt = U_m \sin(\omega t + \theta) \end{cases} \tag{1}$$

Solving Formula (1) yields:

$$i = \frac{\sqrt{2}U_m}{Z}\sin(\omega t + \theta - \varphi) - \left[\frac{U_{C(0)}}{\omega_0 L} + \frac{\sqrt{2}U_m \cos(\theta - \varphi)}{Z\omega\omega_0 LC}\right] e^{-\sigma t}\sin\omega_0 t + \frac{\sqrt{2}U_m \sin(\theta - \varphi)}{Z\sin\alpha} e^{-\sigma t}\sin(\omega_0 t - \alpha) \tag{2}$$

θ is the closing phase angle; U_m is the peak power supply voltage; U_c is the voltage at both ends of the capacitor; $U_{c(0)}$ is the voltage carried by the capacitor before the circuit breaker is put into the circuit, Z is the loop impedance. In fact, due to the small size of the circuit, the calculation of relevant parameters is shown in Formula (3).

$$\begin{cases} Z = \sqrt{(\omega L - \dfrac{1}{\omega C})^2 + R^2} \\ \alpha = \arctan(\dfrac{\omega_0}{\delta}) \\ \varphi = \arctan(\dfrac{\omega L - \dfrac{1}{\omega C}}{R}) \\ \omega_0 = \sqrt{1/LC} \\ \delta = R/2L \\ \varphi = -\dfrac{\pi}{2} \end{cases} \tag{3}$$

If the initial voltage of the capacitor is not taken into account, Formula (2) can be further simplified:

$$i = \frac{\sqrt{2}U_m}{Z}\left[\cos(\omega t + \theta) - \frac{\omega_0}{\omega}\sqrt{\sin^2\theta + \frac{\omega^2}{\omega_0^2}\cos^2\theta}\right] \times \cos\left[\omega_0 t + \arctan\left(\frac{\omega_0}{\omega}\tan\theta\right)\right] e^{-\delta t} \tag{4}$$

Formula (4) indicates that the closing inrush current in a circuit is minimized when the closing phase angle is 0°, and the closing voltage on the busbar reaches zero. This criterion selects the phase for closing, ensuring that the system experiences minimal damage. However, the formula does not consider the residual voltage on capacitors. In practical operation, the AC filter must be switched on frequently to provide reactive power for the converter station and perform harmonic filtering. Switching the AC filter circuit breaker is more frequent than switching the line circuit breaker, and it is exposed to mixed AC and DC voltages during opening and closing. Due to the capacitors' memory effect in the filter, charges accumulated during frequent switching may not be fully discharged, leading to a residual voltage. When not fully discharged, this residual voltage impacts the closing inrush

current of AC filters, thereby affecting the overall system performance.

III. Residual Charge Calculation Model

A capacitor, a fundamental component in electrical engineering, comprises multiple capacitive components that exhibit memory properties, a key characteristic that leads to the generation of residual charges. This crucial aspect can occur through various means, such as the use of internal fuses to disconnect breakdown components within capacitors or the occurrence of local flashover phenomena. The primary focus of this article is on the generation of residual charges. We will concentrate on modeling and analyzing the occurrence of flashover phenomena in capacitors for future research, a topic of significant importance in our field.

As shown in Fig. 2, capacitors C_1 and C_2 are connected in series and connected to the circuit through switch K. Switch K is set to disconnect at the peak power supply voltage, and both capacitors C_1 and C_2 are charged as follows:

$$\begin{cases} U_1 = Q / C_1 \\ U_2 = Q / C_2 \\ U_m = U_1 + U_2 \end{cases} \tag{5}$$

When switch K is turned off, switch K_1, in parallel with C_1, suddenly closes from the off state, allowing the partial release of the charge of C_1 through the closed circuit of K_1 with a magnitude of Q_0. In the presence of a discharge device in the circuit, the charge Q will be completely released, while Q_0 remains unneutralized. The discharge device creates parallel circuits with C_1 and C_2, redistributing Q_0. Subsequently, K_1 is turned off again from a closed state to simulate flashover in some capacitor components. The faulty part is isolated by a fuse, resulting in the capacity of capacitor C_1 becoming C_1'. The charge on C_1' is now Q minus Q_0, while the charge on C_2 remains Q. If the remaining charge Q_0 is not redistributed through the discharge device onto C_1' and C_2, the voltage of C_1' is:

$$\begin{cases} U_1^{'} = (Q - Q_0) / C_1^{'} \approx U_1 - U_0 \\ U_2^{'} = Q / C_2 = U_2 \\ U_1^{'} + U_2^{'} = U_m - U_0 \\ U_0 = Q_0 / C_1^{'} \end{cases} \tag{6}$$

The remaining charges are redistributed on C_1', and C_2 with their respective charge amounts of Q_{01} and Q_{02}, and Q_0=Q_{01}+Q_{02}. At this time, the voltages of C_1', and C_2 are:

$$\begin{cases} Q_{01} = C_1^{'} Q_0 / (C_1^{'} + C_2) \\ Q_{02} = C_2 Q_0 / (C_1^{'} + C_2) \\ U_1^{''} = -Q_0 / (C_1^{'} + C_2) \\ U_2^{''} = Q_0 / (C_1^{'} + C_2) \end{cases} \tag{7}$$

At the maximum Q_0, i.e. when Q_0=Q, C_1' the maximum overvoltage occurs on the capacitor, i.e.

$$U_1^{''} = -Q / (C_1^{'} + C_2) = -U_1 C_1 / (C_1^{'} + C_2) \tag{8}$$

The SC filter, as demonstrated in Table I, has a capacitor parameter of 3.605 μF. The composition method involves 100 series and 4 parallel small capacitors, illustrated in Fig. 3.

The four series capacitors are divided into two parts, with the first group on the left forming the first part and the 99 group on the right forming the second part. The two capacitors are connected in series, with the capacitance sizes as follows:

$$\begin{cases} C_1 = 100C = 3.6 \times 10^{-4}\,\mathrm{F} \\ C_2 = C_1 / (100 - 1) = 3.64 \times 10^{-6}\,\mathrm{F} \end{cases} \tag{9}$$

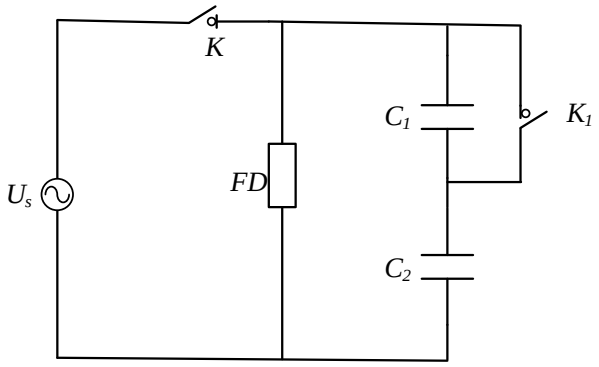

Fig. 2 Model of residual charge generation.

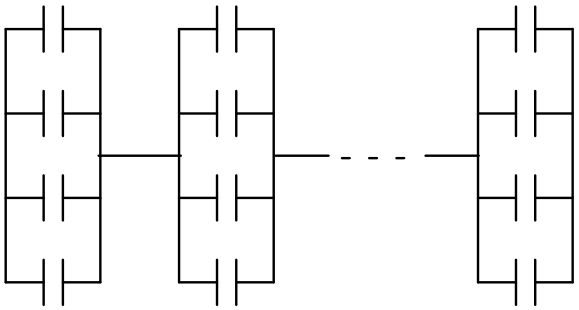

Fig. 3 Schematic diagram of a 100 series 4-parallel capacitor model.

TABLE I
UNBALANCED CURRENT SIMULATION AND THEORETICAL CALCULATION RESULTS

N	I_{TA1}/A	I_{TA2}/A	actual value	theoretical value
0	0	701.5	/	/
1	1.83	701.1	383.11	382
2	3.84	699.8	182.24	182
3	6.04	694.2	114.93	115.33
4	8.44	692.1	82.00	82
5	11.12	690.2	62.07	62
6	14.14	687.1	48.59	48.67
7	17.5	683.9	39.08	39.14
8	21.3	680.4	31.94	32
9	25.7	676.6	26.33	26.44
10	30.58	672.1	21.98	22
11	36.4	666.8	18.32	18.36
12	43.2	660.6	15.29	15.33
13	51.3	653.3	12.73	12.77
14	61.2	644.5	10.53	10.57
15	73.27	633.4	8.64	8.67
16	88.48	619.3	7.00	7
17	108.6	601	5.53	5.53
18	136.42	575.9	4.22	4.22
19	177.5	539.2	3.04	3.05
20	240.43	480.7	2.00	2

Each series capacitor bank consists of four parallel capacitors, and the size of each small capacitor is:

$$C_3 = C_1 / 4 = 9 \times 10^{-5}\,\mathrm{F} \tag{10}$$

If a flashover phenomenon occurs on the capacitor C_1, the internal fuse will act to disconnect the faulty part. After this disconnection, the capacitor will be transformed into C_1' with a modified size.

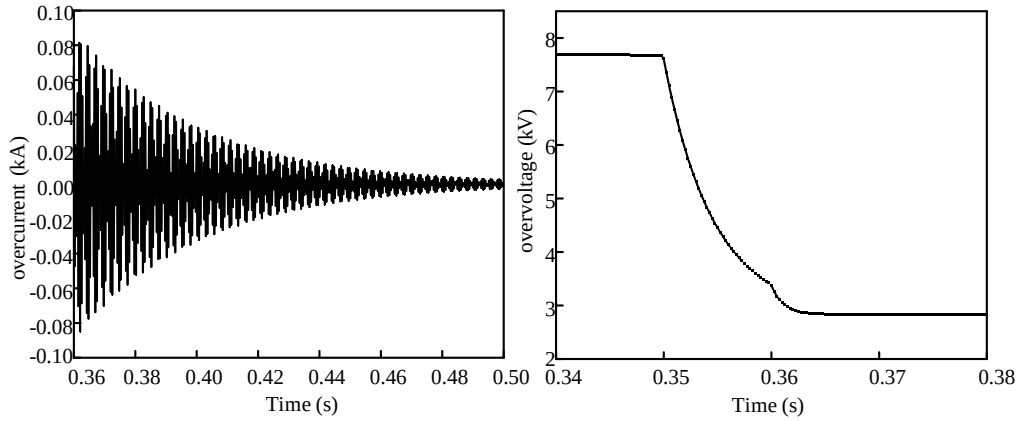

Fig. 4 Overcurrent and overvoltage on capacitors

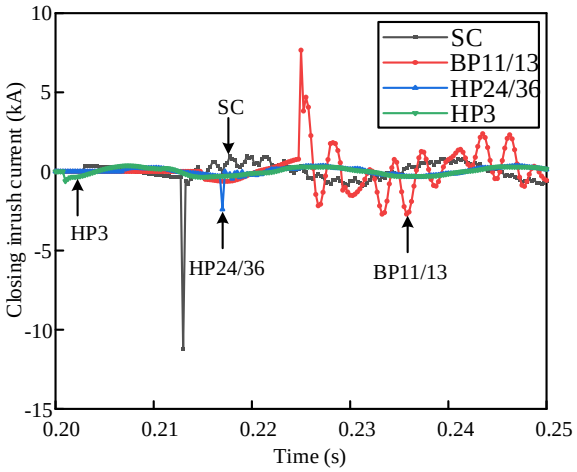

Fig. 5. Maximum overcurrent of four types of filters.1

$$C_1^{'} = 3C_1/4 = 2.7\times10^{-4}\text{F} \tag{11}$$

The line voltage is converted to phase voltage and its peak value is calculated. After calculation and simulation, it is determined that the peak voltage of the filter in the system during regular operation is 612 kV. The initial voltage and charge on capacitors C_1 and C_2 are:

$$\begin{cases} U_1 = U/100 = 6.12\text{kV} \\ U_2 = 99U/100 = 605.9\text{kV} \\ Q_1 = C_1U_1 = 2.2\times10^{-3}\text{C} \\ Q_2 = C_2U_2 = Q_1 = 2.2\times10^{-3}\text{C} \end{cases} \tag{12}$$

After the flashover phenomenon of the capacitor, assuming Q_0=Q, the voltage on C_1 and C_2 is:

$$U_1^{''} = -U_1C_1/(C_1^{'}+C_2) = 8.06\text{kV} \tag{13}$$

The flashover phenomenon is associated with C_1 releasing the maximum charge, resulting in a peak voltage of 8.06 kV on the capacitor due to residual charge. Reconnecting the capacitor with this voltage to the system could affect its operation. Subsequent analysis will investigate and evaluate this impact.

IV. Calculation Results and Discussion of Closing Inrush Current

A. The Surge Impact of Residual Charge on Capacitors

Analyzing the filter, due to the effect of residual charge, the filter will generate a residual voltage of 3.37 kV and a residual current of 85.2 A. Analyzing the capacitors with residual charges in the filter will create a residual voltage of 2.84 kV and a residual current of 42.6 A after being mistakenly connected, as shown in Fig. 4. The following text will provide the impact of closing surge current on the system and the measures to suppress and protect it.

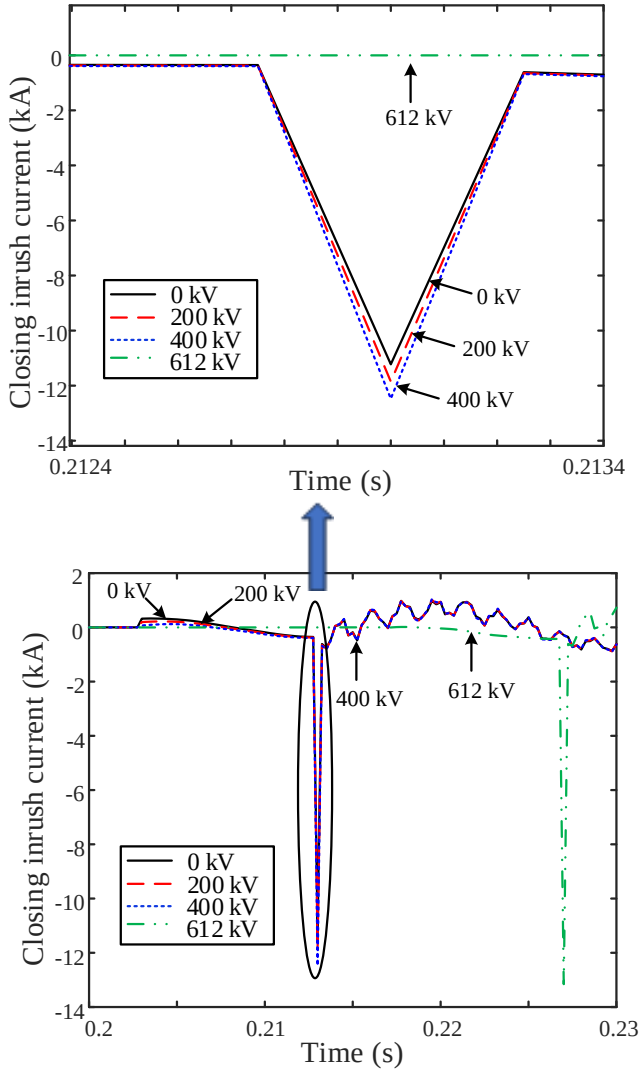

Fig. 6. Maximum closing inrush current of SC filter under different residual voltages.

The analysis is a comprehensive study of the simulation and modeling of a scenario where the AC filter exits the circuit, releasing residual charge on the capacitor inside without connecting to the closing resistor of the converter station system, and the circuit breaker is mistakenly closed. Using the SC filter as an example, the maximum residual

voltage caused by the residual charge on the capacitor inside the filter at the initial state is 8.06 kV. When the SC filter is mistakenly closed at 0.35 s, the remaining charge forms a connected circuit, leading to closing overvoltage and inrush current on the SC filter's external and internal capacitors. The filter, affected by residual charge, generates a residual voltage of 3.37 kV and a residual current of 85.2 A. Capacitors with residual charges in the filter generate a residual voltage of 2.84 kV and a residual current of 42.6 A after being mistakenly connected. The subsequent discussion will focus on the urgent need for measures to suppress and protect against closing surge current on the system.

B. Effect of Residual Voltage on Closing Inrush Current

The closing inrush current of the AC filter in the converter station, as depicted in Fig. 5, was calculated. Upon comparison, it was observed that the closing inrush current produced by the HP3 filter was the smallest, while that generated by the SC capacitor was the largest. This disparity can be attributed to the varying sizes of inductance in the different filters. The inductance L1 of the HP3 filter measured 790.02 mH, whereas the SC capacitor only had an inductance of 2.15 mH. The reason for the overcurrent is the unique internal structure of the SC filter, which exhibits lower inductance and impedance than other AC filters, resulting in a diminished suppression effect on overcurrent. In high-voltage direct current transmission engineering, the system experiences many harmonics due to resonance and the switching of various equipment in the power system. The presence of harmonics often leads to overvoltage and overcurrent, posing a substantial threat to the stability of system operation and diminishing the lifespan of various electrical equipment.

The line voltage is converted into phase voltage, and its peak value is calculated. After calculation and simulation, the peak voltage of the filter in the system during regular operation is determined to be 612 kV. This section delves into the role of residual voltage in the closing inrush current of the filter under different conditions (200 kV, 400 kV, and 612 kV). It compares the inrush current when residual voltage is not considered, providing a clear understanding of this factor's impact on the AC filter's performance. Using the SC filter as an example, Fig. 6 illustrates the closing inrush current under various residual voltage conditions. Without considering residual voltage, the maximum inrush current generated when the AC filter is activated at 0.203 s is 11.22 kA. However, when the residual voltage is 612 kV and the closing phase angle is 324°, the closing inrush current increases to 13.15 kA. This represents a 17% increase in the closing inrush current when residual voltage is considered, highlighting the significant impact of residual voltage on the performance of the AC filter.

The closing inrush current of four types of AC filters under varying residual voltages is illustrated in Fig. 7. The results underscore the importance of understanding the behavior of different AC filters in response to varying residual voltages. Notably, SC filters exhibit the most pronounced changes in closing inrush current as residual voltage increases, while HP24/36 filters demonstrate less variation. The HP3 filter, with the highest internal inductance and capacitance component parameters, shows a significant 143.4% increase in peak closing inrush current compared to the closing inrush current without residual voltage.

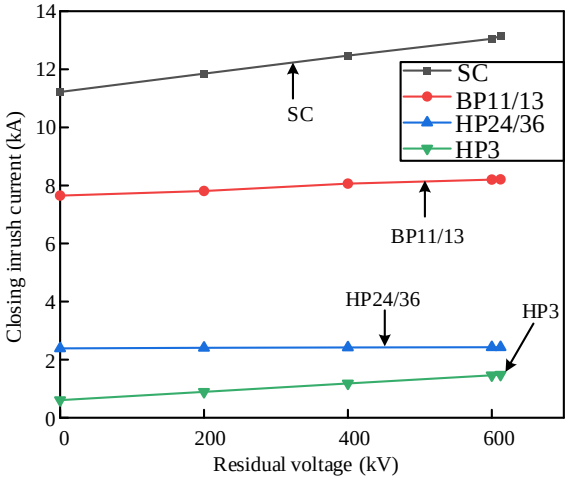

Fig. 7. Peak closing inrush current of four filters under different residual voltages.

V. Measures for Suppressing Closing Inrush Current Considering Residual Voltage Overview of the Model

A. New Adjustable Discharge Resistor

When a flashover fault occurs on the capacitor, it is necessary to troubleshoot it in time to avoid further damage. For the SC filter in this paper, the H-type wiring is used, as shown in Fig.8. As the total capacitance size of the capacitor is 3.605 uF, the capacitor is designed so that:

$$\begin{cases} p_A = p_B = 20 \\ s_A = s_B = 5 \\ p_C = p_D = 20 \\ s_C = s_D = 6 \\ C_e = 1uF \end{cases} \tag{14}$$

From formula (14), P and s represent the number of parallel and series capacitors, respectively; C_e is the capacity of a single small capacitive element; p_A, p_B, p_C, p_D and s_A, s_B, s_C, s_D represent the number of series and parallel connections of capacitors on the bridge arm, respectively.

Assuming that the impedance of TA_1, the midpoint of the bridge arm, is 0, then the unbalanced current flowing between the bridge arms is:

$$I_{TA_1} = \left(\frac{C_A}{C_A + C_B} - \frac{C_C}{C_C + C_D} \right) I_{TA_2} \tag{15}$$

The SC AC filter capacitors are wired in H. C_A, C_B, C_C, and C_D, which are the capacitance capacities of the four bridge arms and are configured precisely for C_A C_B, C_C, and C_D. I_{TA2} is the total current flowing through the AC filter. When the AC filter is regularly operated, there is no current flow between the two bridges, $I_{TA1} = 0$. When the C_A has a small capacitor flashover phenomenon and the internal fuse is part of the fault cut off, there is an unbalanced current between the two bridges, based on the capacitor, which can be identified as a flashover failure. From the above analysis, it can be seen that a bridge arm of the capacitor component failure, the unbalanced current, the failure of the capacitor component, and the total current flowing through the filter size. The unbalanced current calculation formula needs to be derived to

investigate further the change of unbalanced current after the failure of a capacitive element, highlighting the need for thorough analysis in understanding system failures.

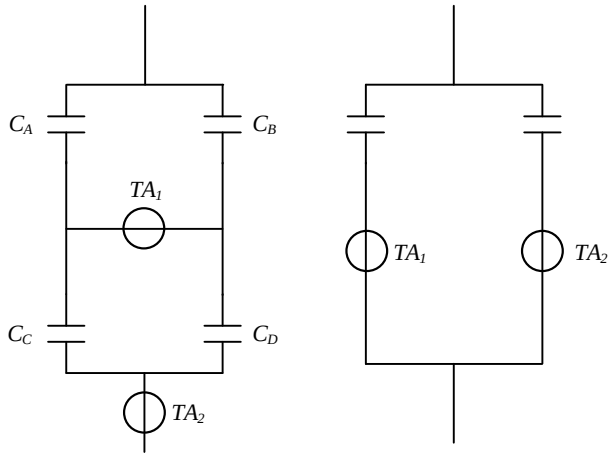

Fig. 8. Schematic diagram of high-voltage capacitor wiring.

Assuming a flashover fault occurs inside the AA bridge arm capacitor, the number of faulty elements is N. The defective component, which the internal fuse can remove, plays a crucial role in maintaining the safety and functionality of the system. The capacitance value of the faulty AA bridge arm is obtained according to the series-parallel relationship of the capacitors and is calculated as:

$$\frac{1}{C_A}=\frac{1}{(p_A-N)C_e}+\frac{1}{p_AC_e/(s_A-1)} \tag{16}$$

The non-faulty bridge arm capacitor capacitance value is:

$$\begin{cases} C_B=\dfrac{p_BC_e}{s_B} \\ C_C=\dfrac{p_CC_e}{s_C} \\ C_D=\dfrac{p_DC_e}{s_D} \end{cases} \tag{17}$$

Substituting and simplifying the above equation yields:

$$\frac{I_{TA_2}}{I_{TA_1}}=\frac{400-18N}{N} \tag{18}$$

From the above equation, it becomes evident that when a fault occurs in the AA bridge arm capacitor, the ratio of the total current to the unbalanced current is solely related to the number of faulted capacitors. This crucial insight allows us to use the ratio of the two as a reliable indicator for the occurrence of flashover faults in the capacitor, thereby providing a practical tool for identifying and addressing such faults in power systems.

Based on the 750 kV AC power supply, the above capacitors are modeled by PSCAD/EMTDC software, the line voltage RMS is 612 kV, the topology of the capacitors is H-type wiring method, and the number of series-parallel connections is as described above. Set the capacitor on the AA bridge arm parallel section capacitance flashover phenomenon after the internal fuse is removed, from 0.2 s moment for the first piece of small capacitance is removed, every 0.5 s to remove a piece of small capacitance, until 0.3 s moment a group of AA bridge arm capacitance in series unit a total of 20 pieces of small capacitance is removed. Fig. 9 records 20 pieces of small capacitance in the gradual occurrence of the flashover failure after removing the internal fuse after the H-bridge. The internal current I_{TA2}, as seen in Fig. 9, the unbalanced current after the fault increases gradually. The unbalanced current grows increasingly with the increase in the number of capacitor slices of the fault.

Table I provides crucial insights into the size of the current and unbalanced current flowing through the external AC filter. These insights are particularly significant as the number of small capacitors cut off by the internal fuse action increases after the flashover of the capacitor's internal capacitance piece. The ratio of the two is then analyzed against the theoretical value obtained by the calculation results of the above formula. The findings are profound, revealing that the difference between the theoretical value and the actual value is insignificant, thus confirming the accuracy of the simulation with a high degree of confidence. As the number of flashover capacitors increases, the unbalanced current between the H-bridges gradually increases, the current flowing through the AC filter slowly decreases, and the ratio decreases gradually. The amplitude of the ratio decreases with the increase in the number of capacitors with flashover faults also decreases gradually. This significant finding allows us to determine how many internal small capacitors have failed when the capacitor's internal flashover fails, based on the ratio of external current and unbalanced current.

On the AA bridge and CC bridge side of the flashover fault, I_{TA1} is for the positive direction; on the BB bridge and DD bridge side of the flashover fault, I_{TA2} is for the negative direction. The process is straightforward: the TA_1 current transformer, equipped with a meter, is the basis for judgment. A positive meter reading indicates a capacitor flashover fault on the AA bridge and CC bridge side, while a reversed reading indicates a fault on the BB bridge and DD bridge side.

$$\begin{aligned} U_{AA}&=U_{BB}=278.6kV \\ U_{CC}&=U_{DD}=334.7kV \end{aligned} \tag{19}$$

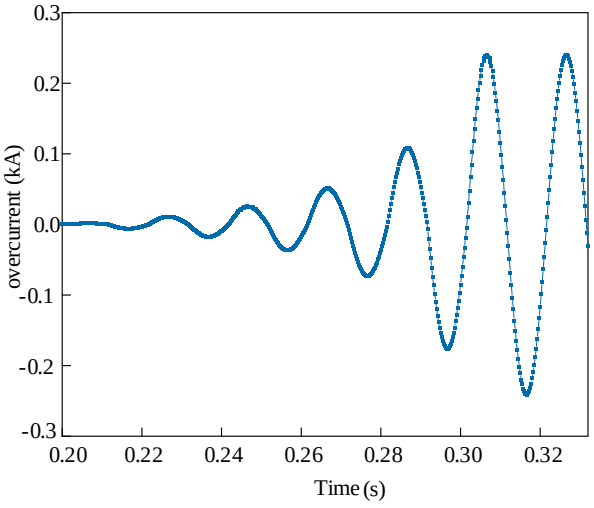

Fig. 9 Gradual flashover removal overcurrent in a 20-piece capacitor.

After simulation analysis can be obtained, if the capacitor does not occur inside the flashover fault, the capacitor's four bridges on the voltage are:

After the gradual removal of 20 small capacitors, the voltage waveforms on the four bridge arms are shown in Fig.

10 and Fig. 11:

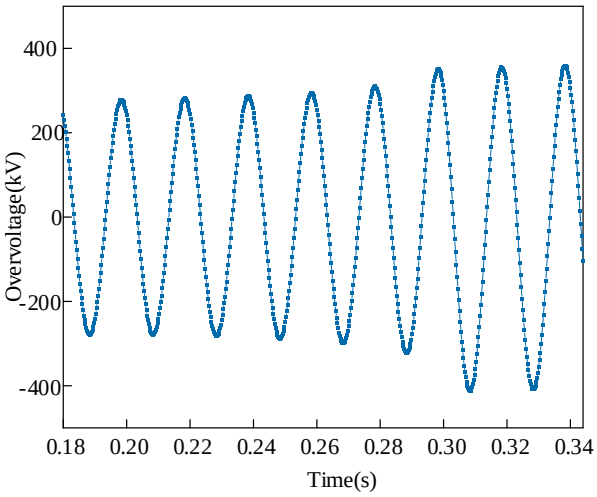

Fig. 10 Overvoltage on AA and BB bridges after gradual flashover removal of the 20-piece capacitor.

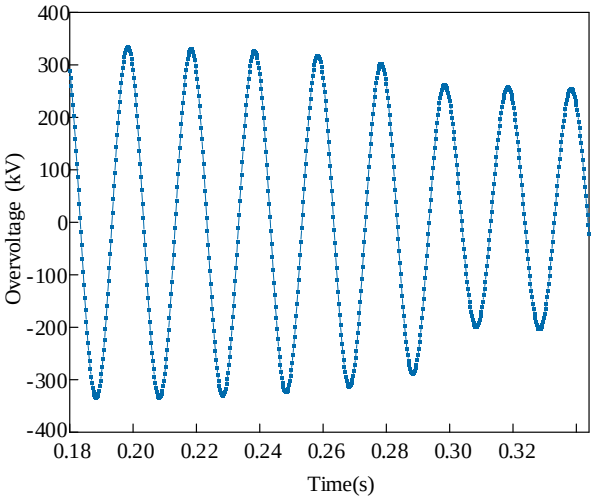

Fig. 11 Overvoltage on the CC and DD bridges after progressive flashover removal of a 20-chip capacitor.

The overvoltage peaks at 0.2 s and 0.3 s, and the nearby peak points are taken out and recorded at the corresponding moments, the ORIGIN software is applied to make two sets of graphs after the least squares fitting of the two data sets. For the two sets of data on the AA bridge and CC bridge, the fourth-order function is fitted to obtain two sets of graphs in Figs. 12 and 13.

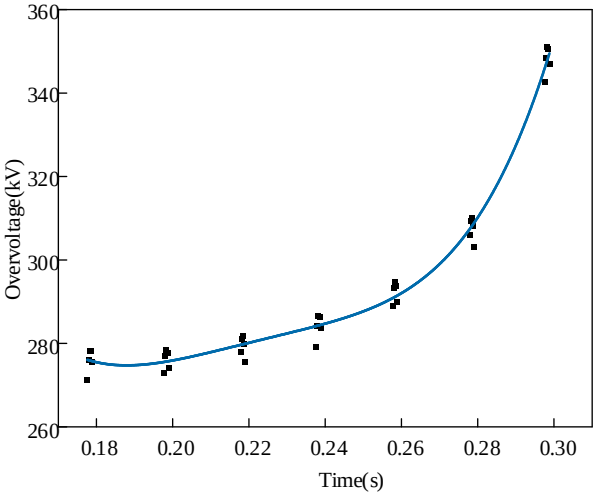

Fig. 12 Peak overvoltage variation for AA and BB bridges

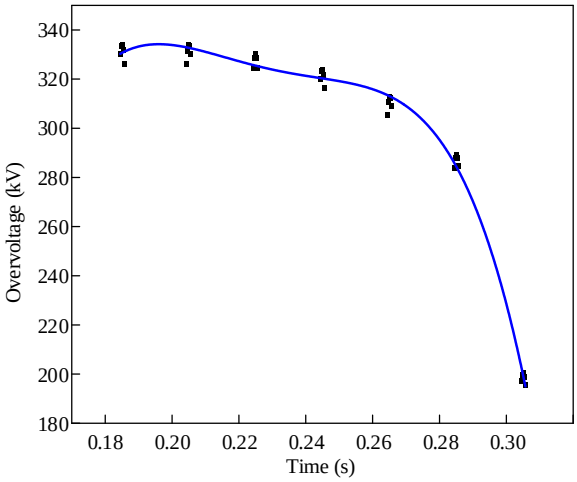

Fig. 13 Peak overvoltage variation for CC and DD bridges

After comparative analysis, it can be seen that after the flashover of 20 pieces of capacitors on the AA bridge and BB bridge in turn, the coefficient of the quadratic function of the fitted curve of the peak voltage is positive, showing a monotonically increasing trend; after the flashover of 20 pieces of capacitors on the CC bridge and the DD bridge, the coefficient of the quadratic function of the fitted curve of the peak voltage is negative, showing a monotonically decreasing trend, so it can be used as a basis for judging that when the peak voltage fitting polynomial is positive, the capacitor flashover fault occurs on the side of the CC bridge and the BB bridge. When the coefficient of the quadratic term of the peak voltage fitting polynomial is positive, the capacitor flashover fault occurs on the AA bridge and BB bridge side; when the coefficient of the quadratic term of the peak voltage fitting polynomial is negative, the capacitor flashover fault occurs on the CC bridge and DD bridge side.

In practical terms, the TA_1 transformer's current direction detection can serve as a reliable criterion for identifying faults on the left and right sides of the H-bridge. Similarly, the increase and decrease of the peak overvoltage fitted curve can be used as a criterion for detecting faults on the upper and lower sides. The imbalance current ratio plays a crucial role in determining the capacitance slices of the flashover capacitor that need to be removed by the inner fuses, thereby streamlining the fault detection and removal process.

B. New Adjustable Discharge Resistor

It is essential to discharge capacitors after use to prolong their lifespan and ensure user safety. Traditional methods of capacitor discharge include natural discharge, where the charge leaks slowly through the insulating medium in the air when there are no external loads, resulting in a gradual and controlled decrease in voltage across the capacitor. This method is not recommended due to its slow discharge speed. Another technique uses discharge resistors, which are fixed resistors that cause the voltage on the capacitor to change over time.

$$\begin{cases} U = U_0 e^{-\tau t} \\ \tau = R_0 C \end{cases} \tag{20}$$

Among them, U0 represents the residual voltage formed by the capacitor during the generating residual charge, while R0

denotes the discharge resistance. The charge on a capacitor exhibits an exponential decay over time, with the rate of decay determined by the time constant. After five cycles in a circuit, denoted by τ, the voltage across the capacitor terminals drops to 1% of the original value, marking the end of the discharge process. It is generally accepted that the discharge process concludes at this point, highlighting the effectiveness of using a discharge resistor. However, the conventional discharge resistor, typically a fixed-value resistor with an unadjustable resistance, has significant drawbacks. These drawbacks include a rapid decrease in discharge current as the process continues due to the constant resistance value, leading to a slower discharge rate.

Consequently, the discharge progress slows down considerably. This article introduces a novel adjustable dynamic discharge resistor that promises significant benefits. The concept is to maintain a relatively high current on the discharge resistor to accelerate the discharge speed, achieved by incorporating a variable resistor. The fastest discharge rate can be achieved by keeping the current at the initial discharge level constant over time. This results in a uniform decrease in the charge on the capacitor over time, offering a more efficient and effective discharge process and reassuring you of its effectiveness.

$$\begin{cases} Q = Q_0 - I_0 t \\ R = R_0 - \dfrac{1}{C} t \end{cases} \tag{21}$$

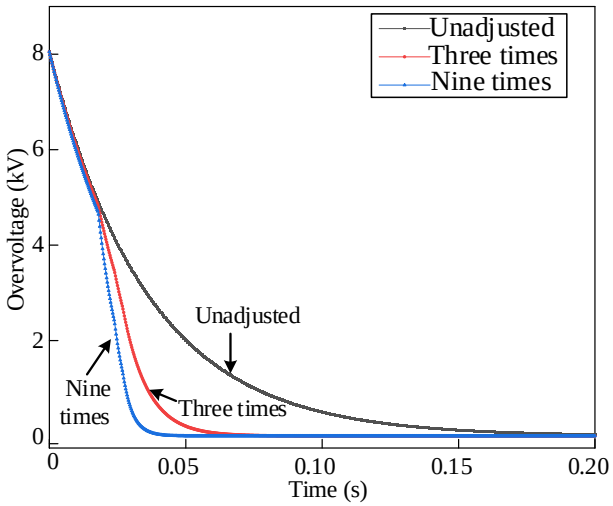

Fig. 15. Variable discharge resistor overvoltage attenuation diagram after 3 and 9 adjustments.

When the equation $t=R_0C$ is satisfied, indicating complete discharge where the resistance is 0, achieved through a short circuit. The relationship between discharge resistance R and time t is linear, with a fivefold increase in discharge rate. By splitting the discharge resistors into smaller units and connecting them in parallel, they are sequentially introduced to the discharge current through a relay device at different discharge stages. The relay device plays a crucial role in this process, as it controls the introduction of the discharge resistors to the discharge current, ensuring a sequential and controlled discharge. As the number of parallel discharge resistors rises, the resistance value decreases, leading to increased discharge current in later stages and a faster discharge rate. Assuming a discharge resistance of 10 kΩ, a time constant of 0.03 s can be calculated. When four discharge resistors are sequentially connected to the circuit at different time points, with resistance values of 10 kΩ, 5 kΩ, 3.3 kΩ, and 2.5 kΩ respectively, the discharge time can be adjusted three times. By increasing the number of adjustments to nine, the total resistance values of the discharge resistors will be 10 kΩ, 5 kΩ, 3.3 kΩ, 2.5 kΩ, 2 kΩ, 1.7 kΩ, 1.4 kΩ, 1.25 kΩ, 1.1 kΩ, and 1 kΩ. Increasing the number of discharge resistors compared to using four times connecting discharge resistors can enhance the precision of the discharge process. Additionally, as the total resistance value of the discharge current decreases after the time interval of the first time constant, the discharge current increases, accelerating the discharge process. Fig. 15 illustrates that after nine adjustments of the discharge resistance, the discharge time approaches 0.03 s, demonstrating a constant discharge rate. This method proves to significantly enhance the discharge rate of the capacitor, effectively guiding the discharge process and providing protection for both the capacitor and the entire system, with a predictable and constant discharge rate.

VI. Conclusion

By meticulously modeling the residual charge and voltage at the Changji converter station, we can accurately calculate the closing inrush current and overvoltage generated by the AC filter. This process has led us to some significant conclusions:

(1) When compared and analyzed with the unaccounted residual voltage, the residual voltage injected into the capacitor reveals some alarming results. At a residual voltage of 612kV, the closing inrush current increases by 17% compared to the unapplied residual voltage. The maximum residual voltage formed by the residual charge on the capacitor is 8.06kV. These findings underscore the potential threat residual charge and voltage can pose to the system's operation, highlighting the critical importance of our research.

(2) When a capacitor experiences a flashover, it's crucial to identify the fault location promptly. This can be achieved by using the H-bridge type wiring, the ratio of the total current and the unbalanced current as the capacitor flashover number of pieces of evidence. The current direction of the TA_1 transformer can be detected by detecting H-bridge faults occurring on the left and right sides of the evidence. The over-voltage peak of the fitting curve of the increase or decrease in the value of the evidence can be used as a failure of the top and bottom of the two sides of the evidence. By integrating these three methods, the capacitor flashover fault systems can be comprehensively and accurately identified, providing a sense of reassurance about the effectiveness of the proposed method.

(3) This paper proposes a novel type of adjustable dynamic discharge resistor, which makes a significant contribution to the field. After nine adjustments of the discharge time close to 0.03s, this resistor can be discharged four times to improve efficiency. This innovation has the potential to significantly enhance the performance of high-voltage systems, instilling a sense of optimism about the field's future.

REFERENCES

[1] T. Fu, Z. Zhang, J. Huang, “Analysis of typical faults in frequent switching of AC filters in converter stations,” Electrotechnical Journal, no. 09, pp. 154-155+159, 2023.

[2] X. Qiao, “Analysis of the causes of DC power reduction caused by continuous removal of AC filters in converter stations,” Electrotechnical Journal, no. 24, pp. 184-187, 2022.

[3] H. Liao, N. Wu, H. Peng, “Method for determining the optimal number of input groups for AC filters in converter stations,” Journal of Shandong University (Engineering Edition), vol. 52, no. 05, pp. 77-83, 2022.

[4] X. Ma, B. Bin, X. Fang, “Research on the optimization strategy for the replacement plan of AC filter field equipment,” Technology Wind, no. 02, pp. 81-83, 2022.

[5] X. Wu, S. Xu, Y. Wang, “Damping high pass filter and its application in high voltage DC systems,” High Voltage Technology, vol. 48, no. 10, pp. 4072-4081, 2022.

[6] X. Li, “Research on overvoltage and insulation coordination of AC filter in ± 800 kV converter station,” South China University of Technology, no. 1, pp. 1-77, 2020.

[7] Y. Wu, J. Guo, “Research on typical fault overvoltage characteristics of ± 1100 kV DC filter,” Power Engineering Technology, vol. 39, no. 01, pp. 130-137, 2020.

[8] C. He, X. Chen, X. Zhu, “Switching inrush current and its suppression method for 750 kV AC filters in converter stations,” Power Grid Technology, vol. 45, no. 08, pp. 3181-3189, 2021.

[9] F. Ma, Z. Xiang, H. Ni, “Simulation of abnormal pre input of closing resistance of 750 kV filter field circuit breaker,” High Voltage Electrical Appliances, vol. 59, no. 06, pp. 65-73+102, 2023.

[10] B. Niu, F. Ma, P. Ding, “Analysis of the closing resistance fault of circuit breakers for 800 kV AC filter fields,” High Voltage Electrical Appliances, vol. 56, no. 07, pp. 36-43, 2020.

[11] Q. Sun, Y. Tu, J. Fu, “Fracture analysis of the fastening bolt for the closing resistor of a 1100 kV GIS circuit breaker,” Zhejiang Electric Power, vol. 42, no. 08, pp. 68-74, 2023.

[12] J. Cheng, “Research on the prediction method for closing resistance fault of circuit breakers used in 750 kV AC filters,” High Voltage Electrical Appliances, vol. 59, no. 08, pp. 239-244, 2023.

[13] P. Xiao, H. Zhang, Z. Du, “Research on the suppression method of excitation inrush current selection and closing for ultra-high voltage converter transformers,” High Voltage Electrical Appliances, vol. 59, no. 05, pp. 146-153+162, 2023.

[14] C. Yao, G. Xu, L. Sun, “Research and design of mechanical stability of phase selection and closing circuit breakers,” High Voltage Electrical Appliances, vol. 58, no. 11, pp. 167-175+183, 2022.

[15] H. Li, B. Liu, W. Teng, “Method for suppressing transformer excitation inrush current based on variable closing angle,” China Electric Power, vol. 55, no. 09, pp. 70-78, 2022.

[16] Z. Gan, R. Zhang, H, Wang, “Analysis of unstable factors in phase selection and closing of high voltage AC circuit breakers,” Electrotechnical Journal, no. 24, pp. 148-151, 2021.

[17] X. Li, J. Zhang, D. Zhang, “Excitation inrush current suppression of ultra-high voltage converter based on phase selection and closing,” Journal of Anhui Electrical Engineering Vocational and Technical College, vol. 26, no. 02, pp. 65-73, 2021.

[18] Z. Mei, Y. He, “Residual Charge in High-Voltage Capacitors,” Power Capacitor Committee of the Chinese Electrotechnical Society, Capacitor Device Subspeciality Committee of the Chinese Society of Electrical Engineering. Proceedings of the 2003 Power Capacitor Society.

[19] H. Futami, "Study on short time charge behavior in pulsed residual charge method for water tree diagnostics of XLPE cables," 2017 International Symposium on Electrical Insulating Materials (ISEIM), Toyohashi, Japan, 2017, pp. 559-562

[20] J. Deng, H. Mu, G. Zhang, S. Matsuoka, A. Kumada and K. Hidaka, "Residual charge distribution of surface leader discharge under positive impulse voltage," IEEE Transactions on Plasma Science, vol. 41, no. 4, pp. 999-1004, April 2013

[21] P. Zhang, B. Li, W. Li and L. Li, "Influence of inhomogeneous residual charges on the stress of filter capacitor components," IEEE Access, vol. 9, pp. 134289-134297, 2021

[22] L. Jiao, W. An, L. Chi, “Study on two capacitive fast discharge methods,” Safety and Electromagnetic Compatibility, no. 03, pp.73-76, 2023.

[23] S. Li, D. Yang, “Simulation calculation and field measurement analysis of 750 kV AC filter in a converter station,” Power Capacitor & Reactive Power Compensation, vol. 41, no. 01, pp. 91-95+101, 2020.

[24] H. Ni, X. Chen, C. He, “Closing transient characteristics of 750 kV AC filter circuit breaker and its suppression measures,” High Voltage Engineering, vol. 48, no. 05, pp. 1846-1854, 2022.